The NMDA Receptor M3 Segment Is a Conserved Transduction Element Coupling Ligand Binding to Channel Opening

Kevin S. Jones, Hendrika M. A. VanDongen, and Antonius M. J. VanDongen

Department of Pharmacology and Cancer Biology, Duke University Medical Center, Durham, North Carolina 27710

Ion channels alternate stochastically between two functional states, open and closed. This gating behavior is controlled by membrane potential or by the binding of neurotransmitters in voltage- and ligand-gated channels, respectively. Although much progress has been made in defining the structure and function of the ligand-binding cores and the voltage sensors, how these domains couple to channel opening remains poorly understood. Here we show that the M3 transmembrane segments of the NMDA receptor allosterically interact with both the ligand-binding cores and the channel gate. It is proposed that M3 functions as a transduction element whose conformational change couples ligand binding with channel opening. Furthermore, amino acid homology between glutamate receptor M3 segments and the equivalent S6 or TM2 segments in K^+ channels suggests that ion channel activation and gating are both structurally and functionally conserved.

Key words: ion channel gating; affinity; efficacy; receptor structure; ligand binding; neurotransmitters; activation mechanism; NMDA receptor

Cation channels consist of multiple domains or subunits arranged around a central ion-conducting pore. The pore-forming regions of K^+ channels and glutamate receptors (GluRs) display significant amino acid sequence conservation (Wo and Oswald, 1995; Wood et al., 1995), suggesting that they have evolved from a common ancestor (Wood et al., 1995). Identification of GluR0, a prokaryotic ionotropic glutamate receptor with a K^+-selective pore (Chen et al., 1999), confirmed this notion and further strengthened the idea that K^+ channels and glutamate receptors are structurally related (Fig. 1*A*). The amino acid sequence of the "missing link" GluR0 allowed us to extend this homology to the transmembrane segment that follows the P region (Fig. 1*B*). In glutamate receptors, this M3 segment contains a nine amino acid sequence (SYTANLAAF) that is highly conserved throughout all members of the family. The alanine at position 8 of this motif is mutated to threonine in the δ_2 glutamate receptor of the *lurcher* mutant mouse (Zhou et al., 1997). Whereas wild-type δ_2 receptors are nonfunctional in heterologous expression systems, the *lurcher* mutation (A654T) results in constitutive activation of the channel and causes neurodegeneration. Introducing the same mutation in the GluR1 AMPA receptor increases agonist potency and converts a competitive antagonist into an agonist (Taverna et al., 2000). Introducing the *lurcher* mutation into AMPA, kainate, and NMDA receptors reduced receptor desensitization and reduced the rate of receptor deactivation (Kohda et al., 2000). Because the M3 segment is not part of the ligand-binding core, these data suggest a role for M3 in channel activation.

The ligand-binding site in glutamate receptor subunits is formed by two domains, S1 in the N terminal and S2 in the M3–M4 linker (Stern-Bach et al., 1994) (Fig. 1*A*). The S1S2 ligand-binding core of GluR2 has been crystallized, with a partial agonist molecule bound to the structure (Armstrong et al., 1998). More recently, additional structures have been obtained for the GluR2 ligand-binding core, including an agonist-free (apo) conformation, conformations with full and partial agonists, and an antagonist-bound conformation (Armstrong and Gouaux, 2000). The S1–S2 structure reveals two lobes connected by a hinge, forming a clamshell-like structure, similar to the bacterial periplasmic binding proteins (Oh et al., 1993). These novel GluR2 structures confirm and extend what was known for the bacterial periplasmic binding proteins, namely that ligand binding induces a conformational change in which the lobes rotate on the hinge and collapse around the ligand. These crystallographic data suggest a model for agonist activation of glutamate receptors (Armstrong and Gouaux, 2000), in which the binding of ligand stabilizes the closed form of the clamshell (Fig. 1*C–E*).

Because glutamate receptors are tetramers (Laube et al., 1998; Rosenmund et al., 1998), functional receptors contain four ligand-binding sites. NMDA receptors are a subtype of glutamate receptor, the activation of which requires binding of the coagonist glycine in addition to glutamate (Johnson and Ascher, 1987). NMDA receptors (NRs) are heteromeric; they are composed of glycine-binding NR1 subunits (Kuryatov et al., 1994; Hirai et al., 1996) and glutamate-binding NR2 subunits (Anson et al., 1998). An analysis of agonist- and antagonist-binding rates suggested that each receptor contains two glycine- and two L-glutamate-binding sites (Benveniste and Mayer, 1991; Clements and Westbrook, 1991). Despite a rather detailed understanding of ligand binding in glutamate receptors and other ligand-gated ion channels, it is not clearly understood how closure of the ligand-binding lobes leads to opening of the channel gate (Colquhoun, 1998). The data presented here demonstrate that the M3 transmembrane segments of the NMDA receptor couple ligand binding to channel gating.

Received May 30, 2001; revised Dec. 19, 2001; accepted Dec. 20, 2001.

This work was supported by National Institutes of Health Grants NS31557 and MH61506 to A.M.J.V. and by a Minority Predoctoral Fellowship in Neuroscience from the American Psychological Association to K.S.J. We thank Dr. John York for his critical reading of the manuscript.

Correspondence should be addressed to Antonius M. J. VanDongen, Department of Pharmacology and Cancer Biology, Duke University Medical Center, P.O. Box 3813, Durham, NC 27710. E-mail: vando005@mc.duke.edu.

 0270-6474/02/222044-10$15.00/0

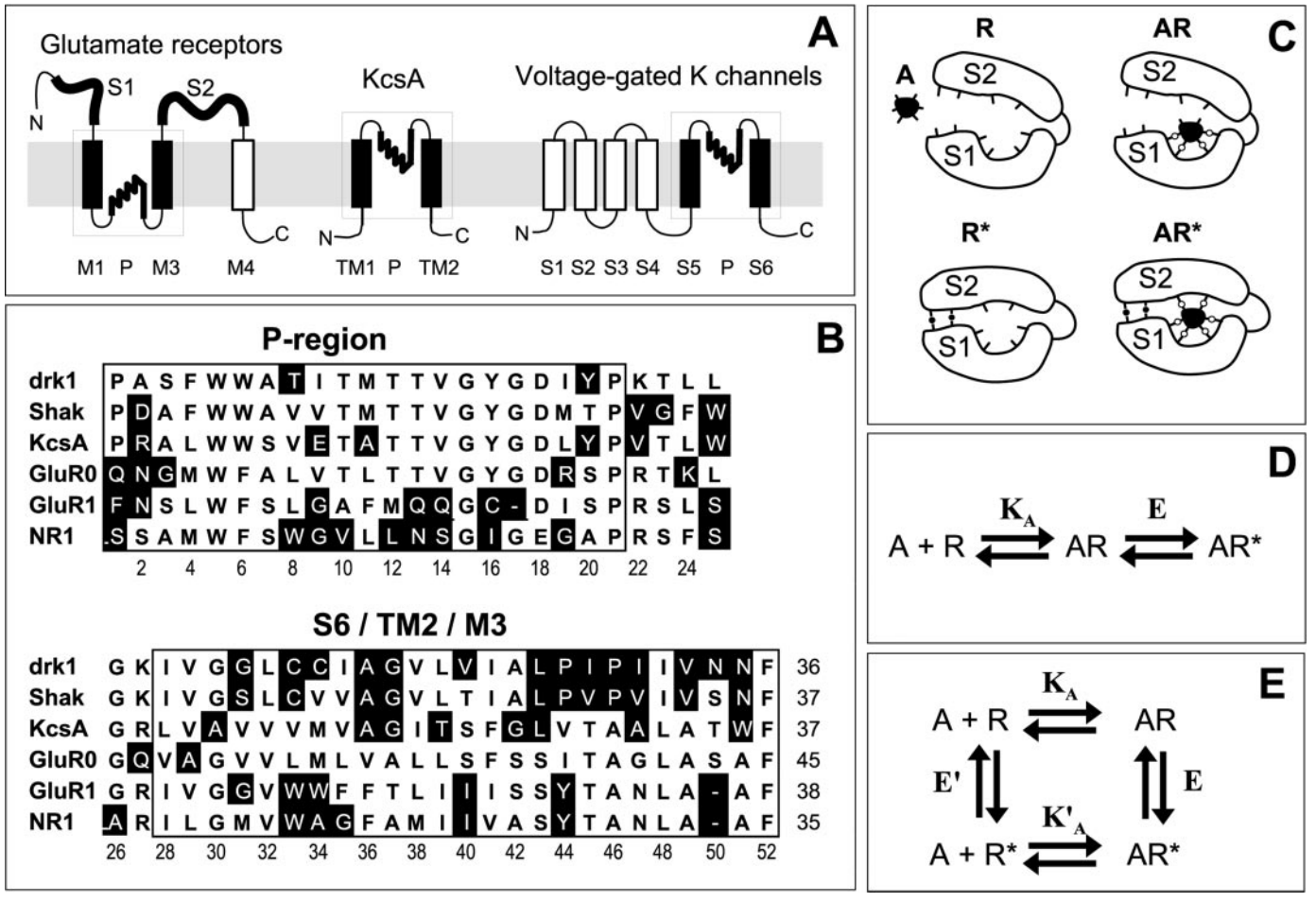

Figure 1. Topology and homology for K^+ channels and glutamate receptors are shown. *A*, Ion channels are modular proteins. The pore-forming region of the bacterial KcsA K channel, formed by two transmembrane segments flanking a re-entrant hairpin loop, represents a motif that is found in both voltage-gated K^+ channels and ionotropic glutamate receptors. *B*, Amino acid sequence alignment of the pore-forming regions and adjacent transmembrane segment for voltage-gated K^+ channels (*P* region plus *S6*), the KcsA K^+ channel (*P* region plus *TM2*), and glutamate receptors (*P* region plus *M3*). Conserved residues are shown on a *white background*. The prokaryotic glutamate-gated K^+ channel GluR0 guides the alignment in the S6–TM2–M3 region. *C*, Schematic representation of four potential conformations of the ligand-binding core of glutamate receptors: the agonist-free conformation (*R*), the agonist-occupied–open conformation (*AR*), the agonist-occupied–closed conformation (*AR**), and the agonist-free–closed conformation (*R**). Crystallographic data exist only for R and AR*. *D*, Linear three-state model of agonist-induced receptor activation. There are two coupled reactions. In the initial association reaction, an agonist binds to lobe S1. In a second step, the agonist-bound conformation can undergo domain closure. The equilibrium constant K_A reflects the affinity of the agonist for the open conformation, whereas *E* is a measure of the agonist efficacy (Colquhoun, 1998). *E*, Allosteric, four-state model of agonist-induced receptor activation (Colquhoun, 1998). The ligand-binding core is able to undergo domain closure in both the absence and the presence of bound agonist. The probability of being in the closed conformation is low in the absence of agonist. Agonist occupancy stabilizes the closed conformation.

MATERIALS AND METHODS

Mutations were generated using the megaprimer PCR method, as described previously (Wood et al., 1995), and were confirmed by DNA sequencing. cRNA for wild-type and mutant NMDA receptor subunits were prepared by *in vitro* transcription, as described previously (Wood et al., 1995).

Oocyte preparation and injection. Adult female *Xenopus laevis* were anesthetized, and a few ovarian lobes containing stage V or VI oocytes were removed. The incision was sutured and the frog was allowed to recover. Oocytes were dispersed by manually disrupting the egg sac and were digested for 2 hr with collagenase type I (2 mg/ml) (Invitrogen, Gaithersburg, MD) to further remove the follicular layer. Injection of cRNA (75 nl of a 10–100 ng/μl solution) was performed under a dissecting microscope with a micrometer-driven micropipetter. Oocytes were then transferred to SOS buffer (in mM: 100 NaCl, 2 KCl, 1.8 $CaCl_2$, 1 $MgCl_2$, 5 HEPES, pH 7.6) supplemented with gentamicin (100 μg/ml) and fungizone (100 μg/ml) and maintained at 19°C.

Two-electrode voltage clamp electrophysiology. Functional expression was assessed 2–5 d after injection using a two-electrode voltage-clamp amplifier (OC-725; Warner Instrument, Hamden, CT) by application of agonists during continuous perfusion of a buffer solution containing (in mM): 100 NaCl, 5 KCl, 0.5 $BaCl_2$, 10 HEPES, 10 μM EDTA, pH 7.3, at 25°C. Barium, rather than calcium, was used as the divalent cation to minimize secondary activation of calcium-activated Cl^- currents (Leonard and Kelso, 1990). EDTA was used to chelate trace amounts of the soft-metal divalent cations Cd^{2+} and Zn^{2+}, which have been reported to contaminate buffer solutions (Paoletti et al., 1997) and inhibit the NMDA receptor by binding to a high-affinity site (Low et al., 2000; Paoletti et al., 2000). EDTA also removes a zinc-dependent component of desensitization (Zheng et al., 2001). Oocytes were placed in a perfusion chamber (Warner Instrument) that was optimized for laminar flow. Solution changes were accomplished using a gravity-fed, computer-controlled perfusion system, which uses BIO-SIL silicone rubber tubing (3.8 mm outer diameter; 1.5 mm inner diameter; Sil-Med, Taunton, MA) and solenoid valves (General Valve, Fairfield, NJ). During solution exchanges, the solution flow rate was ~15 ml/min. Solution exchange kinetics was quantified as follows. Inward NMDA currents were recorded at a holding potential of −60 mV in a buffer containing (in mM) 100 NaCl and 0.5 $BaCl_2$, after application of 10 μM glycine plus 100 μM L-glutamate. When steady state was reached, all of the Na^+ ions were

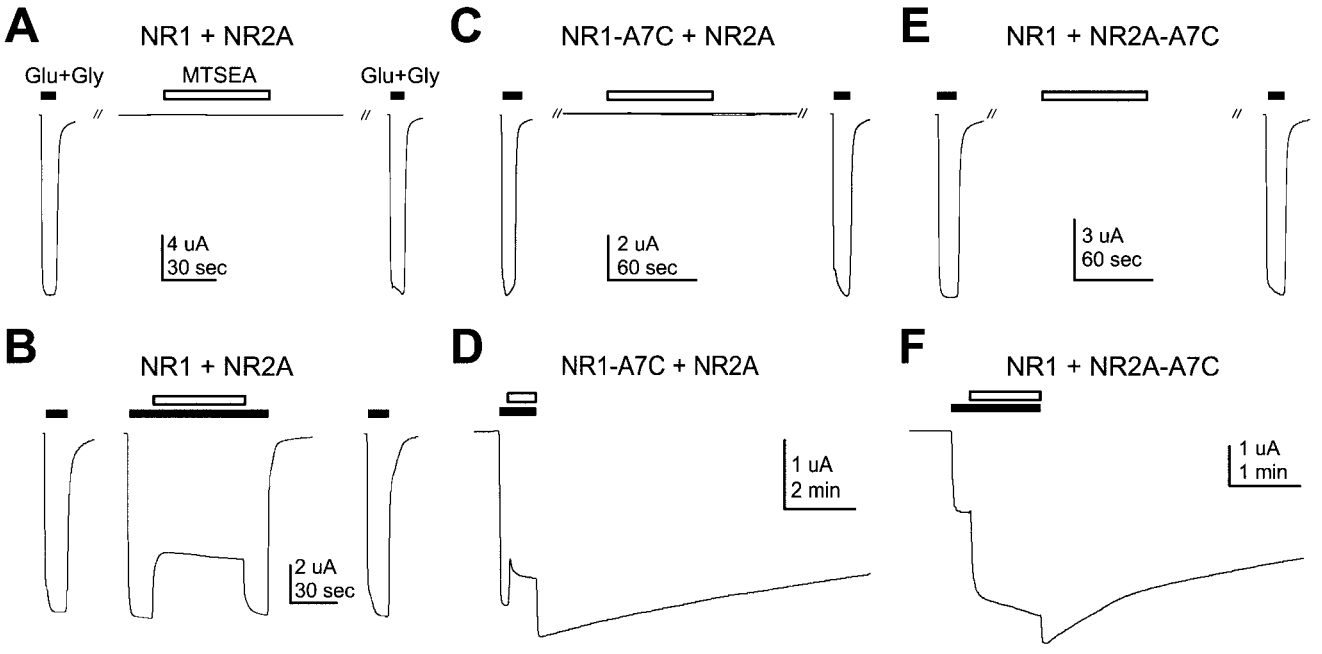

Figure 2. MTSEA modification of A7C-containing receptors is agonist dependent. Representative current traces are shown from oocytes expressing wild-type NR1 plus NR2A NMDA receptors and NMDA receptors containing NR1-A7C or NR2A-A7C subunits, before and after a 60 sec exposure to 0.5 mM MTSEA in the absence (*A, C, E*) or presence (*B, D, F*) of supramaximal concentrations of agonists (100 μM L-glutamate plus 10 μM glycine). *Discontinuous traces* show breaks representing 90–180 sec washout periods. *Dashed lines* represent the maximal response of the oocyte to agonist application before MTSEA treatment. *A*, MTSEA application had no significant effect on the maximal current evoked from wild-type NMDA receptors when applied alone [change in maximal current, $-11 \pm 10\%$ (mean ± SEM); $n = 7$; $p = 0.27$]. *B*, Coapplication of MTSEA and agonists transiently inhibited current from wild-type receptors (change in maximal current, $-43 \pm 5\%$; $n = 4$), although there was no lasting effect on the amplitude of subsequent activation. The change in maximal current was $7 \pm 5\%$ ($n = 4$). *C, E*, MTSEA application did not significantly affect the maximal current evoked from NR2A-A7C or NR1-A7C mutant NMDA receptors when applied in the absence of agonist: the change in maximal current was $-9 \pm 6\%$ ($n = 9$; $p = 0.15$) for NR1-A7C and $-11 \pm 5\%$ ($n = 10$; $p = 0.06$) for NR2A-A7C. ANOVA performed on the data set described in *A*, *C*, and *E* failed to identify a significant difference between the wild-type and A7C-containing receptors ($p = 0.95$). *D, F*, Coapplication of MTSEA and agonists potentiated the agonist-evoked NMDA current and slowed deactivation in A7C-containing receptors (change in maximal current for NR1-A7C, $152 \pm 11\%$; $n = 8$; change in maximal current for NR2A-A7C, $195 \pm 13\%$; $n = 18$).

replaced with impermeable *N*-methyl-D-gluconate ions, resulting in an instantaneous change in the driving force. The inward NMDA current decayed with a biexponential time course. The fast component had a time constant of 180 msec and a relative amplitude of 89%. The remaining 11% decayed with a time constant of 2.3 sec. This implies that ~90% of the solution exchange is complete within 200 msec, but the remaining 10% takes several seconds to complete. Low-resistance glass microelectrodes (0.5–2.0 MΩ) were filled with 3 M KCl and 10 mM HEPES, pH 7.2, and used to impale the oocyte. Current traces were recorded from a holding potential of −60 mV. Data acquisition and voltage control were accomplished with pClamp hardware and software (Axon Instruments, Burlingame, CA).

Curve fitting. The time courses of NMDA current deactivation in Figure 3 were fitted with exponential models by minimizing the residual sum of squares (RSS), using the Solver function in Microsoft Excel (Microsoft, Redmond, WA). One- and two-exponential models were compared using the asymptotic information criterion (AIC) (Akaike, 1981; DiStephano and Landaw, 1984): $AIC = N \log(RSS) + 2P$, where N is the number of data points and P is the number of parameters in the model. The best model is the one that minimizes AIC. The remaining time courses of deactivation and 2-(aminoethyl)methanethiosulfonate hydrobromide (MTSEA) modification were fitted with exponential models using the Clampfit module in pClamp 6.0 (Axon Instruments).

RESULTS

The role of the M3 segment in the activation pathway of glutamate receptors was examined because (1) the *lurcher* phenotype suggested that an M3 residue (A654) had a role in receptor gating and (2) the strict amino acid conservation in the C-terminal half of this transmembrane domain among all of the members of the glutamate receptor family suggested an important functional role. Amino acids in the SYTANLAAF region of NMDA receptor subunits were individually substituted with cysteines. Because functional NMDA receptors are heteromeric assemblies of NR1 and NR2 subunits, mutations were introduced into each subunit separately and coexpressed in *Xenopus* oocytes with the complementary wild-type subunit. NMDA receptors containing mutant subunits were then exposed to the thiol-modifying reagent MTSEA (Akabas et al., 1992) to explore the function of these residues in activation of the receptor. Because both the NR1 and NR2A subunits contain several extracellular cysteines, the effect of MTSEA treatment was first characterized in the wild-type NMDA NR1 plus NR2A receptor.

Effects of MTSEA on wild-type NMDA receptor function

MTSEA treatment of the wild-type NMDA receptors in the absence of agonist had no significant effect on current amplitude (Fig. 2*A*). Simultaneous application of MTSEA and agonists did cause a significant inhibition of NMDA current, but this effect was reversed after washout (Fig. 2*B*). Given its size and charge, it is likely that MTSEA can act as an open channel blocker in NMDA receptors, as has been shown for other channels (Liu and Siegelbaum, 2000). To test this idea, MTSEA was applied at positive holding potentials, where it exerted no effect on current amplitude (data not shown). Therefore, the reversible inhibition by MTSEA in the presence of agonist likely represents open channel block and not covalent modification of a thiol group.

Table 1. Concentration response data for WT, NR1-A7C, and NR2A-A7C[a]

		NMDA current		Modification rate	
Construct	Agonist	EC_{50}	Hill	EC_{50}	Hill
WT	L-glutamate	2.1	0.7	NA	NA
	Glycine	1.5	1.3	NA	NA
NR1-A7C + NR2A	L-glutamate	1.6	1.2	0.6	2.4
	Glycine	0.6	2.4	0.6	1.5
NR1 + NR2A-A7C	L-glutamate	8.2	1.1	3.2	1.1
	Glycine	2.4	1.6	1.9	2.0

[a]Glycine current concentration–response curves were constructed by measuring the peak NMDA response to increasing concentrations of glycine in the presence of 100 μM of L-glutamate. Concentration–response curves for L-glutamate were generated in the presence of 100 μM glycine. Current–response curves to MTSEA modification were similarly constructed by measuring the rate of current potentiation induced by application of the MTSEA to the mutant constructs in the presence of increasing concentrations of one agonist while the co-agonist was held at saturating concentrations. The data were normalized and fit with the Hill equation (see Fig. 5 legend). NA, Not applicable.

Because MTSEA application had no lasting effect on the current amplitude evoked from wild-type NMDA receptors, we conclude that either the endogenous cysteines of the receptor were not available for modification or their modification caused no discernible change in current amplitude.

The SYTANLAAF region

Amino acids in the SYTANLAAF region of NMDA receptor subunits were individually substituted with cysteines. Eight of the nine cysteine-substituted NR1 constructs were functional. However, NMDA receptors containing the NR1-S646C mutation did not yield current. The remaining receptors were exposed to the thiol-modifying reagent MTSEA, both in the absence and in the presence of agonists. Four of the cysteine-substituted NR1 receptors exhibited state-dependent responses to MTSEA application. Simultaneous exposure to MTSEA and agonist reduced the current amplitudes of receptors containing the NR1 mutants T649C, N651C, or L652C by 75 ± 8%, 64 ± 9%, and 40 ± 8%, respectively (data not shown). However, exposure to MTSEA in the absence of agonists did not reduce the NMDA currents in these mutants (data not shown). MTSEA modification of NR1-A653C revealed a critical role in receptor activation. This mutation targets the alanine at position 7 of the SYTANLAAF region and will be referred to as A7C. It should be noted that the A7C mutation immediately precedes the *lurcher* mutation A8T. The remainder of this article characterizes the unique properties conferred by MTSEA modification of NMDA receptors containing the A7C mutation in either the NR1 or NR2 subunit.

Access to residue A7C requires receptor activation

The amplitudes of currents evoked from NMDA receptors containing the A7C mutation in the SYTANLAAF region of either NR1 or NR2A were comparable with that of the wild-type receptor. The glutamate and glycine concentration–response curves of the A7C mutants did not indicate substantial changes in the apparent affinity (EC_{50}) of either of the co-agonists (Table 1). This suggested that the overall structure of the channel was not grossly disrupted by the mutation. NMDA current evoked from receptors containing the A7C mutation in either the NR1 or NR2A subunit was not affected by exposure to MTSEA in the absence of agonist (Fig. 2*C,E*), although simultaneous application of MTSEA and agonists potentiated the current amplitude and markedly decreased the deactivation rate (Fig. 2*D,F*). This indicates a pronounced activation-state dependence for MTSEA modification of the A7C-containing receptors. Similar results were obtained when MTSEA was substituted with the membrane-impermeable analog [2-(trimethylammonium)ethyl] methane thiosulfanate (data not shown), indicating that access to residue A7C occurs from the extracellular space. Taken together, these data suggest that MTSEA gains access to the A7C residue only when the receptor is activated.

MTSEA modification slows deactivation of A7C NMDA receptors

The current evoked during activation of ligand-gated ion channels is rapidly abolished after removal of the agonist. This deactivation occurs as the agonist dissociates from its binding site and the ion channel returns to its resting state. Deactivation of wild-type NR1/NR2A NMDA receptors proceeded with a biexponential time course (Fig. 3). This time course may in part be determined by the relatively slow perfusion system (see Materials and Methods). The deactivation kinetics of A7C-containing NMDA receptors was also biexponential, and the time constants obtained were statistically indistinguishable from the wild-type receptor (Fig. 3). MTSEA application in the absence of agonists did not affect the deactivation kinetics of the wild-type or A7C-containing NMDA receptors. Concurrent application of MTSEA and agonist had no effect on the wild-type NMDA receptor, but it dramatically slowed deactivation of NR1-A7C and NR2A-A7C receptors. Figure 3 summarizes the effects of MTSEA modification on the deactivation kinetics of A7C-containing NMDA receptors, as well as the requirement for the presence of agonists. MTSEA modification also potentiated the amplitude of currents evoked from the A7C NMDA receptors. Interestingly, the potentiation of NMDA current occurred despite activation of the A7C NMDA receptors with supramaximal concentrations of agonists (Fig. 2*D*). The effect that MTSEA exerts on the deactivation kinetics and current amplitudes of the A7C NMDA receptors was examined more thoroughly.

Modification of A7C requires closure of both glutamate- and glycine-binding cores

The experiments described above suggested that activation of the NMDA receptor is required for MTSEA to gain access to the A7C residue. Agonist binding induces receptor activation by a series of conformational changes that culminate in channel opening. This process is initiated by closure of the bilobate binding cores (Armstrong and Gouaux, 2000). In the NMDA receptor, activation requires binding of both glycine and glutamate at the NR1 and NR2A subunits, respectively. Therefore, we investigated whether the application of either co-agonist alone was sufficient to allow MTSEA access to the A7C residue. Coapplication of MTSEA and L-glutamate failed to evoke current from either NR1-A7C- or NR2A-A7C-containing receptors and did not result in their covalent modification (data not shown). However, coapplication of MTSEA and glycine did produce a very slowly developing current in A7C-containing NMDA receptors that required several minutes to reach steady state (Fig. 4). Interestingly, glycine by itself was found to partially activate the NMDA receptor to a level between 1 and 5% of the maximal activation obtained with both co-agonists (Fig. 4). These data suggest that our glycine solutions may have been contaminated by trace amounts of L-glutamate, or alternatively, that glycine may act as a partial agonist at the glutamate-binding site. In both

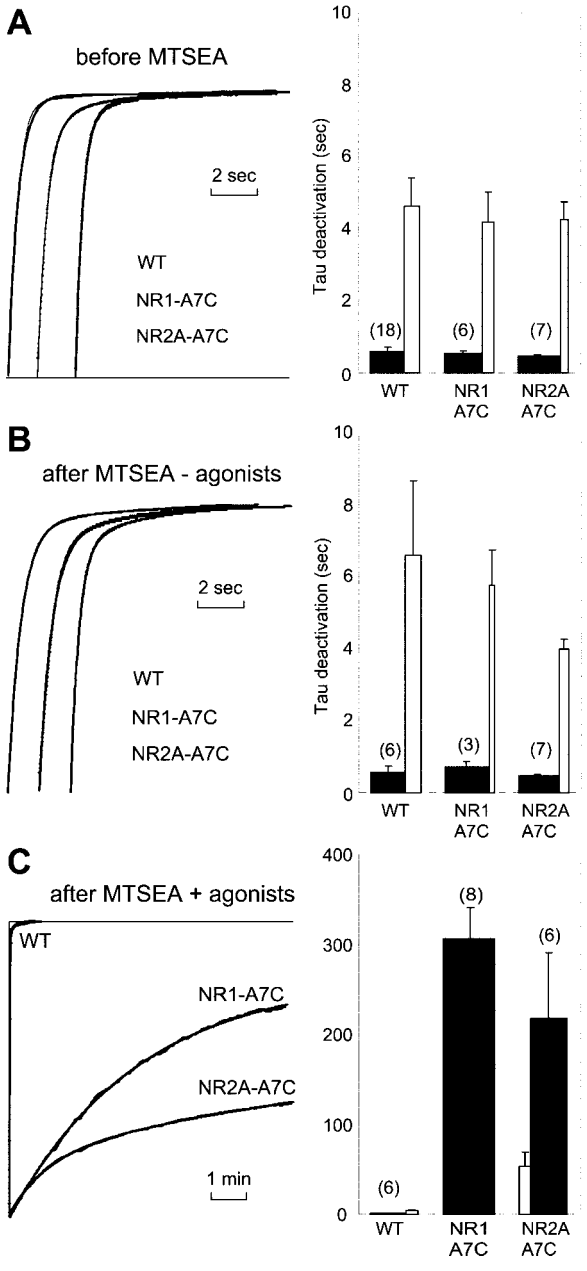

Figure 3. MTSEA modification slows deactivation of A7C receptors. *Left panels*, Representative current traces showing deactivation time course of wild-type (WT) and A7C-containing NMDA receptors before treatment (*A*), after MTSEA treatment (*B*), and after MTSEA treatment in the presence of 10 μM glycine and 100 μM L-glutamate (*C*). To facilitate comparison, the deactivation traces are offset on the time axis and normalized. Exponential fits (*solid lines*) are superimposed on the experimental data. The NR1-A7C trace after MTSEA plus agonists was best described by a single exponential component, whereas all of the other traces required a sum of two exponential components, according to the AIC (see Materials and Methods). The curves in *C* did not return to baseline, and they required an additional offset amplitude. The constitutive activity as a percentage of the maximum MTSEA-modified current was 19% for NR1-A7C and 54% for NR2A-A7C receptors, respectively. *Right panels*, Bar graphs illustrating time constants (means ± SEM) of the exponential models that best describe the deactivation time courses for the three experimental conditions. *Black bars* represent the dominant time constant (that with the largest relative amplitude). The *white bars* represent the time constant with the smallest relative amplitude. The width of each column indicates the relative amplitude of each exponential component; the total width of the black bar plus the white bar represents 100%. Numbers in parentheses represent the number of oocytes.

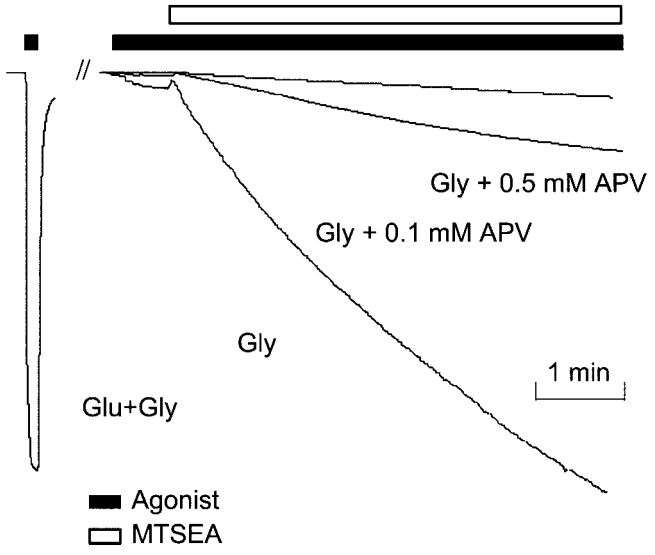

Figure 4. APV prevents MTSEA modification by glycine alone. Representative current traces show modification of NR1-A7C by 0.5 mM MTSEA and 10 μM glycine, in the absence and the presence of 100 or 500 μM APV. Similar results were obtained in NR2A-A7C-containing receptors (data not shown). Traces are normalized to the current amplitude evoked by the supramaximal agonist application represented by the *dashed line*.

scenarios, the glutamate-binding site is partially activated by an agonist. Therefore, we investigated whether the glutamate-binding site plays a critical role in the glycine-only NMDA current, which supports the modification by MTSEA. Coapplication of the competitive L-glutamate antagonist APV reduced the glycine-only currents evoked from the A7C NMDA receptors in a dose-dependent manner (Fig. 4). Concomitant with the reduction in receptor activation, APV also reduced the rate and extent of MTSEA modification observed during glycine application to the A7C NMDA receptors (Fig. 4). Although these results do not fully resolve the nature of the glycine-only currents evoked from A7C-containing NMDA receptors, they indicate that MTSEA modification of A7C requires that both the glycine- and glutamate-binding sites be occupied by effective agonists. The absence of glycine from its binding site or the presence of an antagonist in the glutamate site is sufficient to prevent MTSEA modification.

From the data described thus far, it could be concluded that lobe closure of both the glutamate- and glycine-binding sites is required to allow the conformational change in M3 that makes residue A7C accessible to MTSEA. However, lobe closure at the ligand-binding sites induces a cascade of conformational rearrangements that result in channel opening, Therefore, it is not clear which of the several steps involved directly causes MTSEA accessibility to residue A7C. The conformational change in M3 could result directly from ligand binding, or alternatively, it could be a consequence of channel gating. This point was further elaborated by investigating the correlation between the rate of MTSEA modification with ligand binding and gating parameters. Because thiol modification by MTSEA is extremely rapid, up to 10^5 M^{-1} sec^{-1} (Stauffer and Karlin, 1994), the chemical reaction is not the rate-limiting step of modification. Rather, the rate of MTSEA modification depends critically on the relative amount of time that the cysteine at position A7 is exposed to the aqueous environment of the receptor.

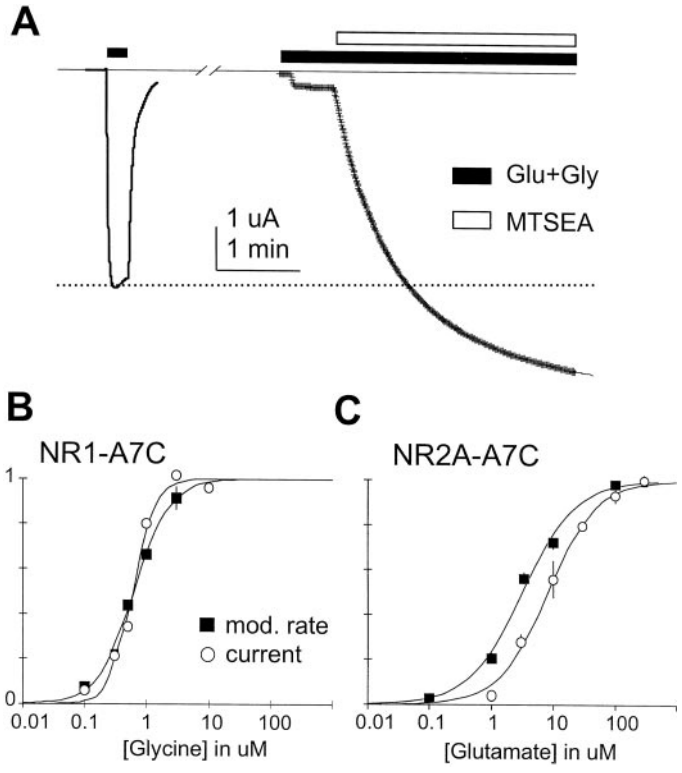

Figure 5. MTSEA modification rate depends on agonist concentration. *A*, Representative NR1-A7C NMDA currents showing the effect of lowering the agonist concentration on the MTSEA modification rate. Supramaximal agonist concentrations (100 μM glutamate plus 10 μM glycine) were first applied to establish the maximal current (indicated by the *dotted line*). A submaximal concentration of glycine (100 μM glutamate plus 100 nM glycine) was then applied, resulting in a fractional response. Addition of 0.5 mM MTSEA resulted in a slowly developing potentiation to a level that exceeded the maximal response before treatment. *B*, Glycine concentration–response curves for NR1-A7C in the presence of a saturating concentration of L-glutamate (100 μM). Graphs are shown for normalized NMDA currents (*open circles*) and normalized MTSEA modification rates (*closed squares*). *C*, Glutamate concentration–response curves for NR2A-A7C in the presence of a saturating concentration of glycine (100 μM). Graphs are shown for normalized NMDA currents (*open circles*) and normalized MTSEA modification rates (*closed squares*). All of the data were fitted with the Hill equation: $R/R_{max} = 1/[1 + (EC_{50}/[\text{agonist}])^n]$, where R is the response (current or rate) for the given agonist concentration, R_{max} is the maximal response, n is the Hill coefficient, and EC_{50} is the concentration midpoint. The values for the Hill coefficient and EC_{50} are listed in Table 1.

MTSEA modification rate depends on agonist concentration

The relationship between MTSEA modification rate and agonist concentration was investigated to correlate the activation state of the A7C NMDA receptors with MTSEA accessibility to residue A7C. When lower concentrations of agonists were used, MTSEA was found to potentiate the NMDA currents substantially (Fig. 5*A*), suggesting that modified receptors are much more sensitive to agonists. The rate of MTSEA modification was much slower when lower concentrations of agonists were used (Fig. 5*A*). The time course of current potentiation was best fit by a single exponential function, and the time constant was dependent on the concentration of both L-glutamate and glycine. However, the MTSEA-induced potentiation of current evoked from the NR2A-A7C receptor became biexponential at the highest agonist concentrations. In all of the cases, the NMDA current potentiation became faster with increasing agonist concentration and the kinetics saturated at higher concentrations. Modification rate constants were plotted as a function of the agonist concentration and fitted with the Hill equation. The resulting half-maximal concentrations (EC_{50}) and Hill coefficients are summarized in Table 1. Normalization of the rate constants allowed for direct comparison between the modification kinetics and the activation state of the NMDA receptor, as reflected by the concentration–response curves (Fig. 5*B,C*). The kinetics of current amplitude potentiation paralleled the concentration-dependent activation of the receptors. The two curves, steady-state activation and MTSEA modification rate, overlapped when plotted as a function of glycine concentration for the NR1-A7C receptors (Fig. 5*B*). However, the MTSEA modification rate curve of the NR2A-A7C receptors was significantly left-shifted from the activation curve when plotted as a function of glutamate concentration (Fig. 5*C*). This discrepancy suggests that A7C accessibility is not directly determined by the activation state (the open probability) of the receptor, as reflected by the normalized concentration–response curve. Instead, the conformational changes in M3 display a differential sensitivity to occupancy at the glycine- and glutamate-binding sites that cannot be derived from channel gating alone.

MTSEA modification of residue A7C depends on agonist efficacy

The recent crystallographic structures of the GluR2 ligand-binding core suggest a model in which interaction of ligands with their binding sites is characterized by two distinct processes, agonist binding and domain closure (Fig. 1*C–E*). These molecular reactions can be described by either a linear three-state model or a more general four-state allosteric model (Colquhoun, 1998). In the linear model, the agonist interacts with the open conformation of the ligand-binding core in an initial binding reaction. Once bound, the agonist stabilizes a closed conformation of the ligand-binding clamshell (Fig. 1*D*). This closed conformation of the ligand-binding core promotes receptor activation and ultimately results in channel opening. In the allosteric model, the ligand-binding core is able to visit the closed conformation spontaneously, even in the absence of bound agonist, although the probability is very low (Fig. 1*E*). However, agonist occupancy facilitates domain closure by stabilizing the closed conformation.

The concentration dependence of the MTSEA modification rate (Fig. 5*B,C*) correlates A7C accessibility with agonist occupancy. However, there are two distinct conformations in which the agonist occupies the ligand-binding core: the agonist-bound–open (A·R) state and the agonist-bound–closed (A·R*) state (Abele et al., 2000). Therefore, we wanted to determine which of these conformations support the accessibility change of residue A7C. This important issue was investigated by activating A7C NMDA receptors with partial agonists before exposure to MTSEA. The models describing the interaction between the agonist and its binding site (Fig. 1*C,D*) are reduced to a two-state scheme at saturating agonist concentrations, in which the probability of observing the unoccupied receptor state(s) becomes vanishingly small. Under these conditions, the ligand-binding cores alternate stochastically between the closed (A·R*) and open (A·R) conformations. The degree of domain closure induced by agonists can vary substantially (Armstrong and Gouaux, 2000) and is an important determinant of the efficacy of the agonist (*E* in Fig. 1*D,E*). Experimentally, agonist efficacy is estimated by its intrinsic activity, α (Ariens, 1954).

By activating A7C NMDA receptors with saturating concen-

trations of agonists with different intrinsic activities, it is possible to correlate the accessibility of residue A7C with the position of the equilibrium between the A·R and A·R* conformations of the ligand-binding core. MTSEA modification of A7C NMDA receptors proceeded more slowly when partial agonists were substituted for L-glutamate or glycine (Fig. 6*A*). Therefore, accessibility of residue A7C, as measured by the rate of MTSEA modification, depends critically on the stability of the agonist-bound–closed conformation (A·R*) of the ligand-binding core. The MTSEA modification rate of the NR1-A7C receptor correlated linearly with the intrinsic activity of the glycine-site agonists, and the modification rate of the NR2A-A7C receptor correlated linearly with the intrinsic activity of the glutamate-site agonists (Fig. 6*B,C*). This could be expected because closure of the NR1 ligand-binding core is induced by glycine and glycine-like compounds, and closure of the NR2 ligand-binding domains are induced by L-glutamate and glutamate-like compounds.

Surprisingly, MTSEA modification of NR2A-A7C receptors also correlated linearly with the intrinsic activity of the agonist bound to the NR1 subunit (Fig. 6*C*). However, modification of the NR1-A7C receptor did not correlate linearly with the intrinsic activity of NR2-bound agonists (Fig. 6*B*). For example, substituting L-glutamate with agonists that have intermediate intrinsic activities did not reduce the rate of MTSEA modification, although substitution with (±)-*cis*-piperidine-2,3-dicarboxylic acid (PDA), a ligand of particularly low efficacy ($\alpha = 0.07$), did result in a significantly slower modification. These data suggest that the access of MTSEA to residue A7C is promoted when the binding sites are in the agonist-bound–closed (A·R*) state. Furthermore, the data revealed a distinct asymmetry in the intersubunit communication between the NR1 and NR2A NMDA receptor subunits, in which the agonist bound at the glycine site exerts a dominant influence over the M3 conformation in its own NR1 subunit as well as the neighboring NR2 subunits.

MTSEA modification increases the efficacy of partial agonists

MTSEA modification of the A7C NMDA receptors increased the current amplitude to levels that were equal to or greater than the responses evoked by full agonists. This occurred in 9 of 10 cases (Fig. 6*D,E*). The current amplitude evoked by the lowest-efficacy glycine agonist, (±)-3-amino-1-hydroxy-2-pyrrolidone (HA-966), was potentiated 70-fold by MTSEA modification. Whereas before modification the relative current amplitudes evoked by partial agonists varied widely, reflecting large differences in intrinsic activity, MTSEA modification potentiated current amplitudes to levels that are much more similar (Fig. 6*D,E*). Therefore, MTSEA modification of A7C NMDA receptors appears to increase the intrinsic activity of partial agonists, converting the majority to full agonists.

DISCUSSION

The data shown here implicate the M3 segment as a critical element in the activation pathway of NMDA receptors. Cysteine substitution of the alanine at position 7 of the SYTANLAAF motif (A7C) revealed agonist-induced accessibility changes. A previous report that studied the same cysteine substitutions (Beck et al., 1999) concluded that none of the positions displayed agonist-dependent accessibility to MTSEA. This apparent conflict can be reconciled by considering the different experimental approaches used. In the present experiments, glutamate and glycine were always coapplied and the buffer used between agonist applications was agonist-free. In the studies performed by Beck et al. (1999), glycine was present throughout the experiment and receptors were activated by the addition of L-glutamate. Consequently, when A7C was treated with MTSEA, it was found that the baseline current slowly increased, which made additional testing difficult. As we have shown, glycine by itself will minimally activate NMDA receptors and permit MTSEA modification, which very slowly increases the size of the current. This modification is prevented by occupying the glutamate-binding site with an antagonist, suggesting that agonist occupancy of both binding sites is required to allow MTSEA access to A7C. Alternatively, it is possible that occupancy of the glycine-binding site is sufficient to activate the receptor partially. In this scenario, the inhibitory effect of APV suggests that glycine binding at the NR1 subunit allows the glutamate-binding core to close in the absence of ligand.

The activation-dependent accessibility of residue A7C does not by itself place M3 in the chain of events that links ligand binding to channel opening. M3 could undergo a conformational change concomitant with channel opening without having a causative role. However, the additional data shown here strongly support the idea that M3 is a transduction element critically involved in coupling ligand binding to channel opening (Fig. 7).

M3 is functionally distinct from the gate

The NMDA receptor is unique among receptors in its dual agonist requirement. Binding reactions at all four subunits allosterically project to a single gate, which "integrates" the information and generates a single output, the open probability. If the accessibility of A7C is completely determined by open probability, then MTSEA modification rate should depend only on the state of activation. However, the modification rate shows a concentration dependence that is distinct (in both its Hill coefficient and its midpoint) from the normalized response curves (Fig. 5, Table 1). Furthermore, the MTSEA modification rate of NR1-A7C is the same for the partial agonist quinolinic acid (QA) and the full agonist L-glutamate, despite that fact that QA activates the NMDA receptor by only 50% (Fig. 6*B*). Therefore, A7C accessibility is not determined strictly by the open probability of the channel. It appears that M3 receives information on events taking place at the glycine- and glutamate-binding sites that cannot be extracted from channel gating alone.

M3 interacts allosterically with the glutamate- and glycine-binding sites

The MTSEA modification rate of A7C-containing NMDA receptors was determined by both agonist concentration and efficacy. Supramaximal concentrations of the full agonists glycine and glutamate, which promote efficient closure of the ligand-binding lobes, permitted rapid modification. Likewise, low concentrations of full agonists or high concentrations of partial agonists, both of which induce infrequent or incomplete domain closure, significantly slowed the rate of modification. These results imply that the activation state of the ligand-binding cores modulates conformational changes in M3 (Fig. 7, *arrow a*). Conversely, M3 also affects the behavior of the ligand-binding lobes, as MTSEA modification of A7C increased the efficacy of the partial agonists. This suggests that MTSEA modification of position A7 in the SYTANLAAF region of the M3 domain alters the interaction between the ligand-binding core and its agonist (Fig. 7, *arrow b*). Introducing a bulky side chain at A7C allosterically shifts the equilibrium between the open and closed cleft conformations.

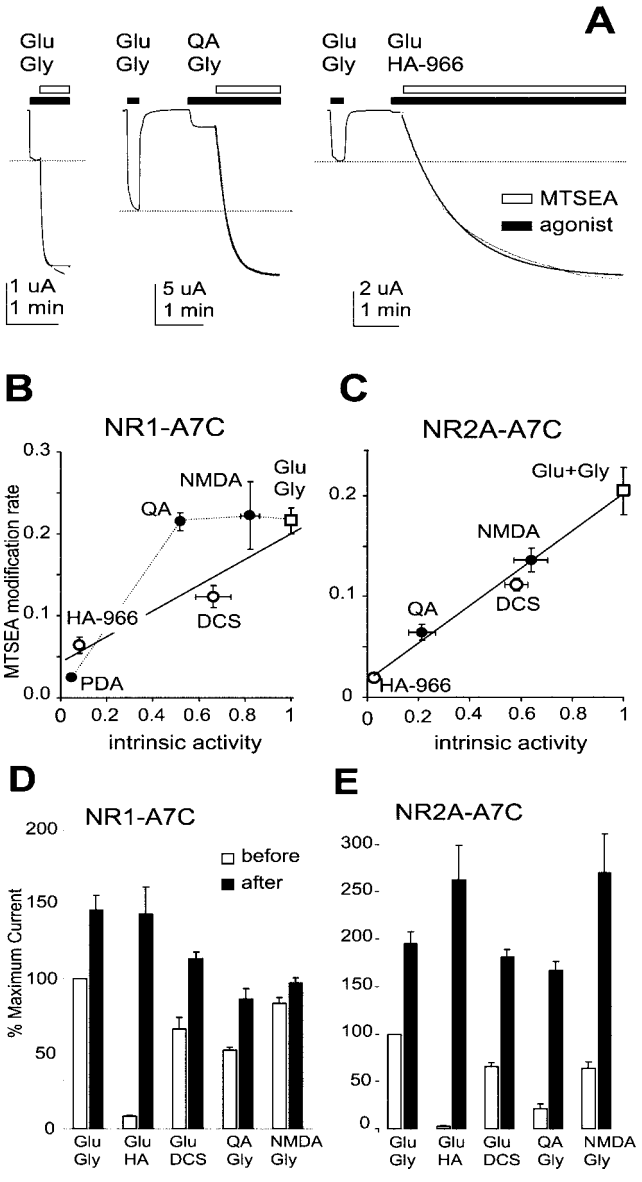

Figure 6. MTSEA modification rate depends on intrinsic activity. *A*, Representative traces show modification of NR2A-A7C in the presence of saturating concentrations of various full and partial agonists. *Left trace*, The full agonists L-glutamate and glycine (100 μM glutamate plus 10 μM glycine) allow rapid modification of the NMDA receptors by MTSEA. *Middle trace*, The partial agonist QA replaced glutamate (5 mM; EC_{50} of 1200 μM and 600 μM for NR1-A7C and NR2A-A7C, respectively). *Right trace*, The partial agonist HA-966 (500 μM) replaced glycine. (Note: the EC_{50} of HA-966 could not be accurately determined, but modification rates were identical at 500 μM and 5 mM, implying saturation of the binding site in NR1-A7C and NR2A-A7C.) *B, C*, Plots of MTSEA modification rate versus agonist intrinsic activity. *Squares* represent modification rates obtained with the full agonists L-glutamate and glycine. *Open circles* represent rates obtained with the partial glycine-site agonists HA-966 (500 μM) or D-cycloserine (100 μM; EC_{50} of 14 μM and 32 μM in NR1-A7C and NR2A-A7C, respectively). *Closed circles* represent rates obtained with the partial L-glutamate agonists QA, NMDA, or PDA. The modification rate for NR1-A7C correlates with the intrinsic activity of the glycine site agonists ($R^2 = 0.926$), but does not correlate linearly with the glutamate site agonists. Modification of NR2A-A7C correlates with both glycine and glutamate site agonists ($R^2 = 0.975$ and 0.982, respectively). Intrinsic activity (α) was calculated as the fraction of maximal current evoked by application of saturating concentrations of partial agonist: $\alpha = I_{\text{partial agonists}}/I_{\text{glutamate + glycine}}$. *D, E*, Bar graphs indicating the fraction of maximal current evoked by each partial agonist before and after MTSEA modification.

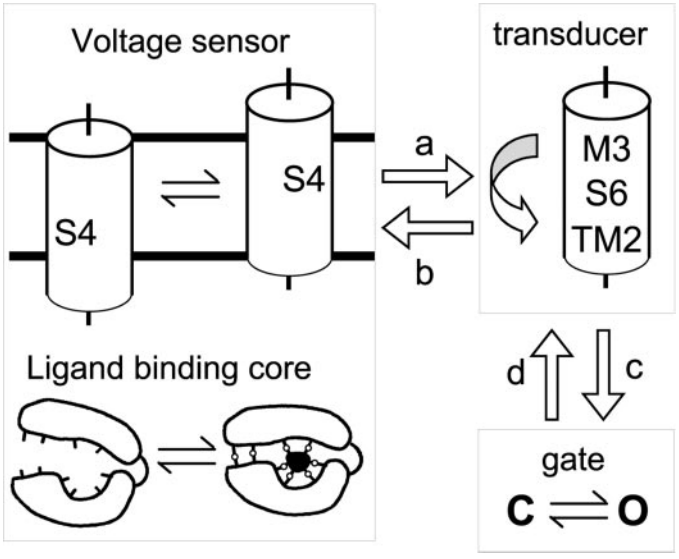

Figure 7. A model for activation of K channels and glutamate receptors and a proposed schematic model of the role of the M3–S6–TM2 segments in channel activation are shown. M3, S6, and TM2 are shown as transduction elements coupling voltage-sensor movement or ligand-binding core closure to the channel gate. *Open arrows* represent allosteric interactions that M3 has with both the ligand-binding core and the gate. Experimental support for three of the four allosteric interactions (*a*, *b*, and *c*) is described in the Discussion.

From this it is concluded that the M3 segments and the ligand-binding cores of NMDA receptors interact through a reciprocal, allosteric mechanism that determines agonist efficacy.

M3 interacts allosterically with the gate

The conformation of M3 affects the behavior of the gate, which is the pore structure directly responsible for opening the channel. MTSEA modification of A7C dramatically affects NMDA receptor gating by decreasing the rate at which the receptor deactivates after agonist removal (Fig. 3*C*). MTSEA modification also results in activation of the NMDA receptor to a level not obtainable by agonists alone (Figs. 2*F*, 6*E*). Taken together, these results suggest that activation of the NMDA receptor evokes conformational changes in the M3 domain, which are then allosterically transduced to affect the behavior of the gate (Fig. 7, *arrow c*). An allosteric interaction between M3 and the gate must necessarily be bidirectional, such that alterations in gating behavior (caused by a mutation or drug) should affect conformational changes in M3 (Fig. 7, *arrow d*). We have not presented data that support this idea.

Cooperativity and asymmetry

The model in Figure 7 schematically illustrates how the M3 segment allosterically mediates the coupling between the ligand-binding core and channel opening. However, the model is incomplete because it shows the ligand-binding site and M3 segment for a single subunit, whereas functional NMDA receptors are most likely tetrameric. Moreover, our results have uncovered a high degree of cooperativity between the movement of the M3 segments in NMDA receptor subunits that needs to be taken into account. Closure of just the glutamate- or glycine-binding lobes is not sufficient to induce the conformational changes in M3 that make residue A7C accessible to MTSEA. However, when both types of binding lobes are closed, MTSEA gains access to residue A7C. This was required whether the cysteine substitution was

introduced in the NR1 or NR2A subunit. The rate of modification of a NR2A-A7C-containing NMDA receptor depended critically on the activation status of both its "own" glutamate-binding core as well as the glycine-binding core localized to the neighboring NR1 subunit. The MTSEA modification of the NR1-A7C receptor was similarly dependent on the conformation of the ligand-binding cores, although the relationship between the modification rate and efficacy for partial glutamate agonists was distinctly nonlinear. This suggests that domain closure of the individual glycine and glutamate bilobate binding cores does not provide enough free energy to induce a conformational change in the M3 segments. Closure of the ligand-binding lobes at both the NR1 and NR2A subunits is required to produce the change in accessibility.

This high degree of cooperativity in the behavior of the M3 segments can be explained by their interaction with a common, single gate (Colquhoun, 1998). Alternatively, the subunits may interact with each other, potentially through the M3 or M1 segments, to produce the cooperativity that was observed. This could also make it easier to explain the asymmetry that has been observed in the interaction between the glutamate- and glycine-binding sites (Benveniste et al., 1990; Lester et al., 1993) (Fig. 6*B,C*).

A conserved transduction element in glutamate receptors and K^+ channels

The M3 domains allosterically interact with both the gate and the ligand-binding sites in the NMDA receptor and mediate their coupling. Ligand binding alters the conformation of M3, which in turn changes the probability that the channel will open. What is the nature of this conformational change that occurs in M3? Data obtained recently for K channels may provide a clue. Pore-forming regions are structurally conserved between ionotropic glutamate receptors and K^+ channels (Fig. 1*A,B*). The glutamate receptor M3 segment corresponds to TM2 in the bacterial KcsA K channel, which has been crystallized recently (Doyle et al., 1998). Electron paramagnetic resonance spectroscopy measurements in KcsA have shown that the α-helical TM2 segment displays rotational and translational movements after activation of the channel (Perozo et al., 1998, 1999). The data presented here are consistent with a similar rotation/translation of the M3 segment underlying NMDA receptor activation.

Furthermore, introduction of a cysteine in the C-terminal half of S6, the equivalent transmembrane segment of the voltage-gated *Shaker* K^+ channel, results in a phenotype very similar to that of A7C in the NMDA receptor. Like A7C-containing NMDA receptors, modification of the S6 cysteine requires channel activation. In addition, deactivation of the *Shaker* K^+ channel was slowed by the presence of soft-metal divalent cations, which can form intersubunit metal bridges (Holmgren and Yellen, 1998). Therefore, we propose that the M3, TM2, and S6 segments are structurally and functionally conserved. They represent universal transduction elements whose translocation couples ligand binding or voltage-sensor movement to channel opening. It therefore appears that glutamate receptors and K channels not only contain structurally highly conserved pore-forming regions but also share a common gating mechanism.

REFERENCES

Abele R, Keinanen K, Madden R (2000) Agonist-induced isomerization in a glutamate receptor ligand-binding domain. J Biol Chem 275:21355–21363.

Akabas MH, Stauffer DA, Xu M, Karlin A (1992) Acetylcholine receptor channel structure probed in cysteine-substitution mutants. Science 258:307–310.

Akaike H (1981) Modern development of statistical methods. In: Trends and progress in system identification. IFAC series for graduates, research workers and engineers, Vol 1 (Eykhoff P, ed), pp 169–184. Oxford: Pergamon.

Anson LC, Chen PE, Wyllie DJA, Colquhoun D, Schoepfer R (1998) Identification of amino acid residues of the NR2A subunit that control glutamate potency in recombinant NR1/NR2A NMDA receptors. J Neurosci 18:581–589.

Ariens EJ (1954) Affinity and intrinsic activity in the theory of competitive inhibition. Arch Int Pharmacodyn Ther 99:32–49.

Armstrong N, Gouaux E (2000) Mechanisms for activation and antagonism of an AMPA-sensitive glutamate receptor: crystal structures of the GluR2 ligand binding core. Neuron 26:165–181.

Armstrong N, Sun Y, Chen GQ, Gouaux E (1998) Structure of a glutamate-receptor ligand-binding core in complex with kainate. Nature 395:913–917.

Beck C, Wollmuth LP, Seeburg P, Sakmann B, Kuner T (1999) NMDAR channel segments forming the extracellular vestibule inferred from the accessibility of substituted cysteines. Neuron 22:559–570.

Benveniste M, Mayer ML (1991) Kinetic analysis of antagonist action at *N*-methyl-D-aspartic acid receptors: two binding sites each for glutamate and glycine. Biophys J 59:560–573.

Benveniste M, Clements J, Vyklicky Jr L, Mayer ML (1990) A kinetic analysis of the modulation of *N*-methyl-D-aspartic acid receptors by glycine in mouse cultured hippocampal neurons. J Physiol (Lond) 428:333–357.

Chen GQ, Cui CH, Mayer ML, Gouaux E (1999) Functional characterization of a potassium-selective prokaryotic glutamate receptor. Nature 402:817–821.

Clements JD, Westbrook GL (1991) Activation kinetics reveal the number of glutamate and glycine binding sites on the *N*-methyl-D-aspartate receptor. Neuron 7:605–613.

Colquhoun D (1998) Binding, gating, affinity and efficacy: the interpretation of structure-activity relationships for agonists and of the effects of mutating receptors. Br J Pharmacol 125:924–947.

DiStephano III JJ, Landaw EM (1984) Multiexponential, multicompartmental, and noncompartmental modeling. II. Data analysis and statistical considerations. Am J Physiol 246:R665–R667.

Doyle DA, Cabral JM, Pfuetzner RA, Kuo A, Gulbis JM, Cohen SL, Chait BT, Mackinnon R (1998) The structure of the potassium channel: molecular basis of K conduction and selectivity. Science 280:69–76.

Hirai H, Kirsch J, Laube B, Betz H, Kuhse J (1996) The glycine binding site of the *N*-methyl-D-aspartate receptor subunit NR1: identification of novel determinants of co-agonist potentiation in the extracellular M3–M4 loop region. Proc Natl Acad Sci USA 93:6031–6036.

Holmgren M, Yellen G (1998) The activation gate of a voltage-gated K channel can be trapped in the open state by an intersubunit metal bridge. Neuron 21:617–621.

Johnson JW, Ascher P (1987) Glycine potentiates the NMDA response in cultured mouse brain neurons. Nature 325:529–531.

Kohda K, Wang Y, Yuzaki M (2000) Mutation of a glutamate receptor motif reveals its role in gating and δ2 receptor channel properties. Nat Neurosci 3:315–322.

Kuryatov A, Laube B, Betz H, Kuhse J (1994) Mutational analysis of the glycine-binding site of the NMDA receptor: structural similarity with bacterial amino acid-binding proteins. Neuron 12:1291–1300.

Laube B, Kuhse J, Betz H (1998) Evidence for a tetrameric structure of recombinant NMDA receptors. J Neurosci 18:2954–2961.

Leonard JP, Kelso SR (1990) Apparent desensitization of NMDA responses in *Xenopus* oocytes involves calcium-dependent chloride current. Neuron 4:53–60.

Lester RAJ, Tong G, Jahr CE (1993) Interactions between the glycine and glutamate binding sites of the NMDA receptor. J Neurosci 13:1088–1096.

Liu J, Siegelbaum SA (2000) Change of pore helix conformational state upon opening of cyclic nucleotide-gated channels. Neuron 28:899–909.

Low C-M, Zheng F, Lyuboslavsky P, Traynelis SF (2000) Molecular determinants of coordinated proton and zinc inhibition of *N*-methyl-D-aspartate NR1/NR2A receptors. Proc Natl Acad Sci USA 97:11062–11067.

Oh B-H, Pandit J, Kang C-H, Nikaido K, Gocken S, Ferro-Luzzi Ames G, Kim S-H (1993) Three-dimensional structures of the periplasmic lysine/arginine/ornithine-binding protein with and without ligand. J Biol Chem 268:11348–11355.

Paoletti P, Ascher P, Neyton J (1997) High-affinity zinc inhibition of NMDA NR1-NR2A receptors. J Neurosci 17:5711–5725.

Paoletti P, Perin-Dureau F, Fayyazuddin A, Le Goff A, Callebaut I, Neyton J (2000) Molecular organization of a zinc binding N-terminal modulatory domain in a NMDA receptor subunit. Neuron 28:911–925.

Perozo E, Cortes DM, Cuello LG (1998) Three-dimensional architecture and gating mechanism of a K^+ channel studied by EPR spectroscopy. Nat Struct Biol 5:459–469.

Perozo E, Cortes DM, Cuello LG (1999) Structural rearrangements underlying K^+-channel activation gating. Science 285:73–78.
Rosenmund C, Stern-Bach Y, Stevens CF (1998) The tetrameric structure of a glutamate receptor channel. Science 280:1596–1599.
Stauffer DA, Karlin A (1994) Electrostatic potential of the acetylcholine binding sites in the nicotinic receptor probed by reactions of binding-site cysteines with charged methanethiosulfonates. Biochemistry 33:6840–6849.
Stern-Bach Y, Bettler B, Hartley M, Sheppard PO, O'Hara PJ, Heinemann SF (1994) Agonist selectivity of glutamate receptors is specified by two domains structurally related to bacterial amino acid-binding proteins. Neuron 13:1345–1357.
Taverna FA, Xiong ZG, Brandes L, Roder JC, Salter MW, MacDonald JF (2000) The lurcher mutation of an alpha-amino-3-hydroxy-5-methyl-4-isoxazolepropionic acid receptor subunit enhances potency of glutamate and converts an antagonist into an agonist. J Biol Chem 275:8475–8479.
Wo ZG, Oswald RE (1995) Unraveling the modular design of glutamate-gated ion channels. Trends Neurosci 18:161–168.
Wood MW, VanDongen HMA, VanDongen AMJ (1995) Structural conservation of ion conduction pathways in K channels and glutamate receptors. Proc Natl Acad Sci USA 92:4882–4886.
Zheng F, Erreger K, Low CM, Banke T, Lee CJ, Conn PJ, Traynelis SF (2001) Allosteric interaction between the amino terminal domain and the ligand binding of NR2A. Nat Neurosci 4:894–901.
Zhou J, DeJager PL, Takahashi KA, Jiang W, Linden DJ, Heintz B (1997) Neurodegeneration in Lurcher mice caused by mutation in delta2 glutamate receptor. Nature 388:769–773.